Polarized Raman Spectra of Oriented Fibers of *A* DNA and *B* DNA: Anisotropic and Isotropic Local Raman Tensors of Base and Backbone Vibrations

George J. Thomas, Jr.,* James M. Benevides,* Stacy A. Overman,* Toyotoshi Ueda,‡ Koichi Ushizawa,‡ Masaaki Saitoh,‡ and Masamichi Tsuboi§

*Division of Cell Biology and Biophysics, School of Biological Sciences, University of Missouri-Kansas City, Kansas City, Missouri 64110 USA; ‡Department of Chemistry, Meisei University, Hodokubo, Hinoshi, Tokyo 191; and §Department of Fundamental Science, Iwaki-Meisei University, Iwaki, Fukushima 970, Japan

ABSTRACT   Polarized Raman spectra of oriented fibers of calf thymus DNA in the *A* and *B* conformations have been obtained by use of a Raman microscope operating in the 180° back-scattering geometry. The following polarized Raman intensities in the spectral interval 200–1800 cm^{-1} were measured with both 514.5 and 488.0 nm laser excitations: (1) I_{cc}, in which the incident and scattered light are polarized parallel to the DNA helical axis (*c* axis); (2) I_{bb}, in which the incident and scattered light are polarized perpendicular to *c*; and (3) I_{bc} and I_{cb}, in which the incident and scattered light are polarized in mutually perpendicular directions. High degrees of structural homogeneity and unidirectional orientation were confirmed for both the *A* and *B* form fibers, as judged by comparison of the observed Raman markers and intensity anisotropies with measurements reported previously for oligonucleotide single crystals of known three-dimensional structures. The fiber Raman anisotropies have been combined with solution Raman depolarization ratios to evaluate the local tensors corresponding to key conformation-sensitive Raman bands of the DNA bases and sugar-phosphate backbone. The present study yields novel vibrational assignments for both *A* DNA and *B* DNA conformers and also confirms many previously proposed Raman vibrational assignments. Among the significant new findings are the demonstration of complex patterns of *A* form and *B* form indicator bands in the spectral intervals 750–900 and 1050–1100 cm^{-1}, the identification of highly anisotropic tensors corresponding to vibrations of base, deoxyribose, and phosphate moieties, and the determination of relatively isotropic Raman tensors for the symmetrical stretching mode of phosphodioxy groups in *A* and *B* DNA. The present fiber results provide a basis for exploitation of polarized Raman spectroscopy to determine DNA helix orientation as well as to probe specific nucleotide residue orientations in nucleoproteins, viruses, and other complex biological assemblies.

INTRODUCTION

Structural features of nucleic acids in biological assemblies are often interpreted in relation to the high-resolution x-ray structures obtained from oligonucleotide single crystals. To investigate native chromosomal structures directly and to advance our understanding of the biological roles of DNA and RNA in supramolecular assemblies, sensitive probes applicable to aqueous solutions and noncrystalline aggregates of the nucleic acids are also required. One method of promise is Raman spectroscopy (Thomas and Tsuboi, 1993). The Raman approach can provide definitive information about covalent bonding configurations and is also potentially informative of electrostatic, hydrophobic, and hydrogen-bonding interactions involving specific nucleotide subgroups. A particular strength of the method is its applicability over a wide range of sample morphologies. For example, Raman spectroscopy has been employed to determine struc-

tures, interactions, and dynamics of viral chromosomes in native virion assemblies (Aubrey et al., 1992; Li et al., 1993a, b) and to map DNA conformation along eukaryotic chromosomes (Puppels et al., 1994). An essential requirement for exploitation of Raman spectroscopy in such studies is unambiguous assignments for the Raman vibrational bands. The structural value of the data may be further enhanced, particularly for applications to oriented macromolecules and symmetrical assemblies, when the local Raman tensors are known beforehand. At present, however, the shape of the Raman tensor is not known for any vibrational band in the spectrum of a macromolecular nucleic acid. In this work, we have measured the polarized Raman spectra of oriented fibers of both *A* DNA and *B* DNA, and we have employed the experimental measurements to determine local Raman tensors of key conformation-sensitive Raman bands assignable to base and backbone moieties of DNA.

The specific goals of this investigation are twofold. First, we seek to identify Raman bands that exhibit highly anisotropic Raman tensors and that therefore can serve as indicators of nucleic acid conformation or subgroup orientation in supramolecular assemblies. As a corollary to this objective, we seek also to identify highly isotropic Raman tensors that can serve as spectral intensity standards, irrespective of the geometric relationship between the electric vector of exciting radiation and the configuration of bonded atoms in

oriented assemblies. Second, we wish to exploit the polarized Raman spectra to resolve and interpret individual band components within complex spectral bandshapes of DNA and RNA, particularly those that have not been amenable to resolution and assignment in unpolarized Raman spectra of nucleic acids.

Previous applications of Raman spectroscopy in nucleic acid research, reviewed recently by Thomas and Tsuboi (1993), have focused on the analysis of Raman frequencies and intensities in unpolarized spectra to reach structural conclusions. Band assignments and interpretations in these earlier studies have been facilitated by a number of empirical approaches including analogy with spectra of mononucleotide (Nishimura et al., 1986) and oligonucleotide single crystals (Thomas and Wang, 1988) of known structure; determination of vibrational frequency shifts accompanying the stable isotope substitutions $^1H \rightarrow {}^2H$ (D), $^{14}N \rightarrow {}^{15}N$, $^{16}O \rightarrow {}^{18}O$ and $^{12}C \rightarrow {}^{13}C$ (Szczesniak et al., 1983; Barnes et al., 1984; Susi et al., 1973; Hirakawa et al., 1985; Delabar and Majoube, 1978; Guan et al., 1994); determination of effects of pH, temperature, and ionic composition on the vibrational frequencies and intensities (Lord and Thomas, 1967; Small and Peticolas, 1971; Stangret and Savoie, 1992); and determination of Raman excitation profiles, which correlate the Raman band intensities with laser excitation wavelengths (Tsuboi et al., 1987). These experimental approaches have also been aided by normal coordinate calculations in which force constants have been transferred from *ab initio* molecular orbital calculations (Tsuboi et al., 1987).

The present paper extends the scope of the Raman methodology by describing procedures for evaluation of the local Raman tensors of *A* and *B* conformers of DNA. For this study, experiments were carried out in parallel at the School of Biological Sciences, University of Missouri-Kansas City, and at the Department of Chemistry, Meisei University.

METHODS

Raman tensors and depolarization ratios

In the off-resonance Raman effect visible laser excitation is employed to excite the Raman spectrum and each spectral band intensity is determined by the change of polarizability associated with the corresponding molecular normal mode. The intensity of each band may be expressed in terms of the elements, α_{xx}, α_{yy}, and α_{zz}, of the derived polarizability tensor ("Raman tensor"). The derivatives are taken with respect to the normal coordinate, and x, y, and z are the principal axes of the tensor. In the absence of molecular symmetry, the principal axes will be oriented differently for each of the $3N$–6 normal modes (N = number of atoms/molecule), and the relative magnitudes of α_{xx}, α_{yy}, and α_{zz} will also generally differ for each mode.

Our specific objectives are to determine the following for each DNA normal mode that generates a Raman band of significant intensity: (1) the orientations of the principal axes (x,y,z) of the Raman tensor with respect to the local molecular geometrical framework; and (2) the relative magnitudes of the Raman tensor components. We

define the latter as

$$r_1 \equiv \alpha_{xx}/\alpha_{zz} \qquad (1a)$$

$$r_2 \equiv \alpha_{yy}/\alpha_{zz} \qquad (1b)$$

The Raman depolarization ratio (ρ), which is defined for molecules oriented randomly in solution, is the ratio of intensities of scattered beams polarized along directions perpendicular ($I_\perp$) and parallel ($I_\parallel$) to the direction of polarization of the exciting radiation. A detailed examination of ρ values for Raman bands of the principal nucleotides of RNA and DNA has been reported recently (Ueda et al., 1993). The depolarization ratio is given in terms of r_1 and r_2 by Eq. 2 (Tsuboi et al., 1991)

$$\rho \equiv \frac{I_\perp}{I_\parallel} \qquad (2)$$

$$= \frac{1.5\{(r_1 - r_2)^2 + (r_2 - 1)^2 + (1 - r_1)^2\}}{5(r_1 + r_2 + 1)^2 + 2\{(r_1 - r_2)^2 + (r_2 - 1)^2 + (1 - r_1)^2\}}$$

The relationship of ρ to r_1 and r_2 can be conveniently visualized using a contour map such as that shown in Fig. 1. The contour map is useful for determining a pair of r_1 and r_2 values consistent with an observed value of ρ. The map is also helpful in locating the principal axes of a given Raman tensor for a molecule in the crystal when appropriate polarized Raman data are available (Tsuboi et al., 1991; Benevides et al., 1993).

Derivation of local Raman tensors for DNA fibers

We choose a rectangular coordinate system (X,Y,Z) fixed on one of the nucleotide units of an oriented DNA fiber so that Z is parallel to the fiber axis (c) and X and Y are perpendicular to c. The Raman tensor of a given vibration
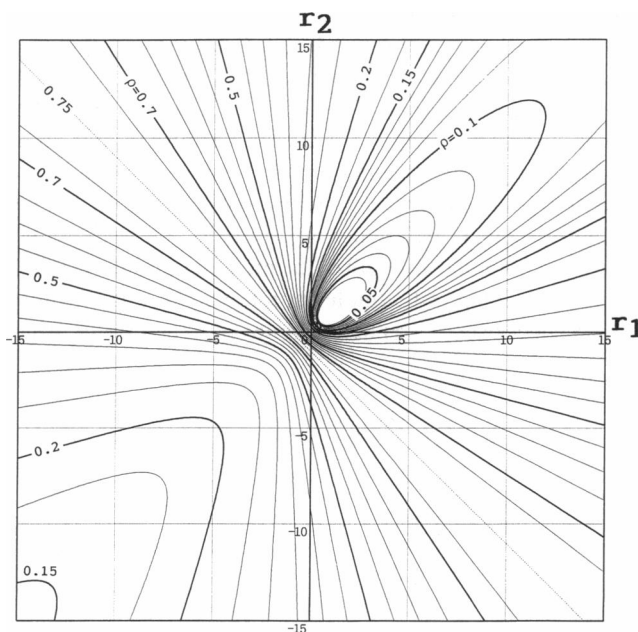

FIGURE 1   Contour diagram relating the Raman depolarization ratio (ρ) of a randomly oriented molecule or molecular subgroup to the parameters r_1 (ordinate) and r_2 (abscissa), as defined in Eqs. 1a and 1b, respectively.

localized in the nucleotide unit is characterized by the three components, α_{xx}, α_{yy}, and α_{zz}, defined above. The Raman tensor components (α_{XX}, α_{YY}, α_{ZZ}) in the **XYZ** coordinate system may be expressed in terms of those of the **xyz** system by Eq. 3, a–f,

$$\alpha_{XX} = l_x^2\alpha_{xx} + l_y^2\alpha_{yy} + l_z^2\alpha_{zz} \tag{3a}$$

$$\alpha_{YY} = m_x^2\alpha_{xx} + m_y^2\alpha_{yy} + m_z^2\alpha_{zz} \tag{3b}$$

$$\alpha_{ZZ} = n_x^2\alpha_{xx} + n_y^2\alpha_{yy} + n_z^2\alpha_{zz} \tag{3c}$$

$$\alpha_{XY} = l_x m_x\alpha_{xx} + l_y m_y\alpha_{yy} + l_z m_z\alpha_{zz} \tag{3d}$$

$$\alpha_{YZ} = m_x n_x\alpha_{xx} + m_y n_y\alpha_{yy} + m_z n_z\alpha_{zz} \tag{3e}$$

$$\alpha_{XZ} = l_x n_x\alpha_{xx} + l_y n_y\alpha_{yy} + l_z n_z\alpha_{zz} \tag{3f}$$

where l_i, m_i, and n_i are the direction cosines of the principal axis i (= x, y, or z) of the local Raman tensor in question.

Because the **X**, **Y**, **Z** coordinates of each nucleotide unit are located along a helical axis, it is convenient to introduce the complex coordinates:

$$a_+ = (X + iY)/\sqrt{2} \tag{4a}$$

$$a_- = (X - iY)/\sqrt{2} \tag{4b}$$

$$a_0 = Z \tag{4c}$$

In terms of these coordinates, the Raman tensor components form the Hermitian matrix of Eq. 5,

$$\begin{bmatrix} \alpha_{++} & \alpha_{+-} & \alpha_{+0} \\ \alpha_{-+} & \alpha_{--} & \alpha_{-0} \\ \alpha_{0+} & \alpha_{0-} & \alpha_{00} \end{bmatrix} = \begin{bmatrix} a_0 & a_2 & a_1 \\ a_2^* & a_0 & a_1^* \\ a_1^* & a_1 & a_{0'} \end{bmatrix} \tag{5}$$

in which the asterisk indicates the complex conjugate, and where

$$a_0 = (\alpha_{XX} + \alpha_{YY})/2 \tag{6a}$$

$$a_{0'} = \alpha_{ZZ} \tag{6b}$$

$$a_1 = (\alpha_{ZX} + i\alpha_{YZ})/\sqrt{2} \tag{6c}$$

$$a_2 = (\alpha_{XX} - \alpha_{YY} + 2i\alpha_{XY})2 \tag{6d}$$

As shown by Higgs (1953), the Raman selection rules and polarization intensities for the helical residues are governed by the relations listed in Table 1. In accordance with this table, the Raman scattering intensities I_{bb}, I_{cc} and I_{bc} (= I_{cb})

TABLE 1 Raman selection rules and intensities for a helical molecule

Polarization				
Incident	Scattered	Symmetry	Phase angle*	Intensity
c	c	A	0	$(a_0)^2$
b	b	A	0	$(a_0)^2$
a	b	E_2	2Ψ	$\frac{1}{2}|a_2|^2$
c	b	E_1	Ψ	$|a_1|^2$
b	c	E_1	Ψ	$|a_1|^2$

*For the A and B DNA helices, $\Psi \approx 33$ and $36°$, respectively.

are obtained as:

$$I_{bb} = (\alpha_{XX} + \alpha_{YY})^2/4 \tag{7}$$

$$I_{cc} = \alpha_{ZZ}^2 \tag{8}$$

$$I_{bc} = (\alpha_{ZX}^2 + \alpha_{YZ}^2)/2 \tag{9}$$

Materials

Calf thymus DNA (lot no. QC814562) was purchased from Pharmacia LKB Biotechnology, Piscataway, NJ. The Raman spectrum of this preparation showed no significant contamination with protein, as evidenced by the absence of Raman bands due to aromatic side chains and invariance of the Raman spectrum to phenol extraction. A stock solution of DNA was prepared at a concentration of 10 μg/μl in 5 mM NaCl, with a final solution pH of 7. This stock solution was used for preparation of fibers. All other reagents were obtained from Sigma Chemical Co. (St. Louis, MO).

Sample handling for Raman spectroscopy

An aliquot of DNA stock solution was concentrated to a gel by evaporation and fibers were drawn from a drop of the gel using a standard fiber-pulling device. Fiber thickness was about 200 ± 20 μm. Fibers were mounted in a thermostatically controlled hygrostatic chamber (microsample cell), which was designed specifically for the sample platform of the Raman microscope (Fig. 2). The microsample cell was constructed from an octagonally shaped (25 mm diagonal) glass slide, onto which was mounted a cylindrical collar (3 mm height × 13 mm diameter), which was drilled to accept the diametrically opposed glass rods of the fiber pulling device. Further details of this Raman microsampling apparatus have been described (Benevides et al., 1993). Sample orientation was checked either by observing the birefringence of the fiber in a polarizing microscope with crossed Nichols optics, or by verification of the high Raman anisotropies expected for bands established previously as originating from in-plane vibrations of the bases (Benevides et al., 1993).

For maintaining the DNA fiber in either the A or B form, the relative humidity (RH) was controlled in the sample chamber with a saturated solution of either NaClO₃ (75% RH) or sodium tartrate (92% RH), respectively. Samples were preequilibrated in the hygrostat for 2 to 10 days at room temperature before spectroscopic analysis. Polarized Raman spectra of the DNA fibers were augmented by depolarization ratio measurements on aqueous B DNA. Solution spectra were obtained on calf-thymus DNA dissolved to 37 μg/μl in 5 mM NaCl at pH 7.

Based upon the examination of a large number of fibers drawn at both the U.S. and Japan laboratories over the several years encompassing this study, the spectra presented below are representative of the greatest degrees of unidirectional orientation and structural homogeneity achievable using the methods employed. The measured Raman anisotropies indicate that the distributions of molecular helical axes in the
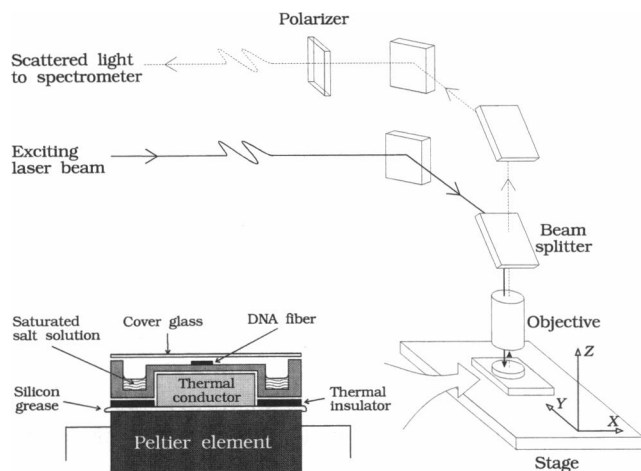
FIGURE 2 Diagram of the Raman microscope employed in this work. The indicated coordinate system (X,Y,Z) defines directions of the electric vectors of incident and scattered laser radiation and the axis of the DNA fiber. Also illustrated is the custom designed Raman cell for maintaining oriented DNA fibers at constant temperature and constant relative humidity. The central portion of the disk-shaped cell consists of an elevated, optically flat glass window upon which the DNA fiber is mounted. Before excitation of the Raman spectrum, the orientation of the fiber can be conveniently examined in a polarizing microscope by directing the polarized light upward through the bottom window. For Raman measurements, constant temperature was maintained by placing the cell upon a thermostated metal cylinder in contact with the bottom window. Constant relative humidity was maintained by placing an appropriate saturated salt solution in the peripheral well.

A and B DNA fibers are within the limits $\pm10°$ and $\pm25°$, respectively, when compared with the true crystallographic c axis of the oriented single crystal of Z DNA examined previously (Benevides et al., 1993).

In our experience, as well as in the experience of others (Brandes et al., 1989), the Raman spectra of A DNA fibers invariably give evidence of admixture with a small amount of B DNA. The present spectra are no exception. However, the degree of such structural heterogeneity is small, usually <30% and presumably indicative of domains (e.g., $(dA)_n \cdot (dT)_n$ sequences) which do not succumb to the B → A transition, irrespective of the salt environment and relative humidity. In the present work, this intrinsic property of A DNA is dealt with by various means. Where feasible, we have employed curve-decomposition of complex band profiles exhibiting weak but authentic B markers (such as the 682 cm^{-1} marker of C2'-endo/anti dG) in order to remove such markers prior to measurement of experimental anisotropies and computation of Raman tensors. In other cases, the weak B markers are sufficiently well resolved instrumentally to exclude them without data refinement from the experimental measurements and calculations. However, in some instances the weak B markers cannot be eliminated altogether. In such cases, the Raman tensors of A DNA should be regarded as "effective" tensors, which are subject to further refinement when polarized spectra of perfectly oriented and conformationally pure A DNA single crystals become available.

Instrumentation for Raman microspectroscopy

Spectra of DNA fibers were obtained on Raman microscope instrumentation in laboratories at the University of Missouri-Kansas City and Meisei University, employing 514.5 and 488.0 nm excitations, respectively. The fundamental design features of these Raman microspectrometers have been described (Benevides et al., 1993; Tsuboi et al., 1991).

The UMKC instrument combines an Olympus microscope (Lake Success, NY, model BHSM) and computer-controlled, triple spectrograph (Edison, NJ, ISA/Jobin-Yvon Model S3000) with an ISA Spectraview-2D charge-coupled device (CCD) detector (1024×256 pixels). Before laser excitation of the Raman spectrum, the thermostated fiber (8°C) was examined with an $10\times$ objective (Olympus NEO S Plan) and assessed for degree of orientation by cross-polarization viewing. With the fiber still in focus of the optical microscope, the 514.5 nm line from a Coherent Innova (Santa Clara, CA) 70-2 argon laser was directed through the objective and onto the sample. The Raman scattering at 180° was collected with an Olympus ULWD MS Plan $80\times$ objective. The radiant power of the laser was maintained at or below 200 mW at the laser head (<15 mW at the sample).

Spectra of DNA solutions were obtained on a scanning double-spectrometer system (Spex Ramalog V/VI, Edison, NJ) under the control of an IBM microcomputer. Details of the instrumentation and sample handling for solution Raman spectroscopy have been described (Li et al., 1981).

At Meisei University, a Jasco R-MPS-22 Raman microscope (Tokyo, Japan) was used. Before Raman spectroscopy, DNA fibers in the custom designed cell (Fig. 2) were examined in a polarizing microscope by sending white light upward through the fiber from the bottom. Raman spectra were excited with the 488.0 nm line of an Ar$^+$ laser (NEC GLG 3300) using a $50\times$ Olympus objective. By cooling the Peltier plate on which the cell was placed, the sample temperature was maintained below 10°C which prevented overheating of the sample by the condensed laser beam. The radiant power of the laser was maintained below 50 mW at the laser head. The Raman scattered beam was collected at 180° with the same objective used to focus the incident beam. The scattered light was then directed by means of a beam splitter to the Jasco NR-1100 Raman spectrophotometer system.

Data collection and analysis

In a typical data collection protocol, the electric vector of the exciting radiation was directed along the laboratory X axis, as defined in Fig. 2. A polarizer located before the entrance slit of the monochromator selects for Raman scattering along either the X axis or perpendicular to it (Y axis) (Benevides et al., 1993). Since the transmittance characteristics of the analyzing polarizer are different for the two orientations, a correction factor based on the transmittance of white light through the system was applied. Differences in detector sensitivity for different CCD channels were also corrected by white light calibration. To minimize optical polarization artifacts, the different Raman polarizations were obtained

by rotating the fiber rather than the electric vector of the radiation. The fiber axis of the sample was placed either along the X or Y axis, as shown in Fig. 2. The Raman intensities were thus measured in the cc (I_{cc}), bb (I_{bb}), bc (I_{bc}) and cb (I_{cb}) configurations. Depolarization ratios were obtained from aqueous solutions of DNA as described previously (Benevides et al., 1993).

Raman spectra were collected over the 200–1800 cm^{-1} region. The data shown below are unsmoothed averages of 6–10 exposures obtained with an integration time of 120 s/exposure and with a spectral resolution of $\sim$6 cm^{-1}. Data collection was accomplished with ISA/Jobin-Yvon software operating on an IBM microcomputer. Processing of the spectral data, including decomposition of complex bandshapes, was accomplished with commercial software for curve fitting (Spectra Calc, Galactic Industries) and custom-designed deconvolution software (Thomas and Agard, 1984). Gauss-Lorentz product functions were generally employed in band-decomposition procedures.

RESULTS AND DISCUSSION

Polarized Raman spectra of A DNA and B DNA fibers

Polarized Raman spectra (I_{bb}, I_{cc}, I_{bc}, and I_{cb}) of A DNA and B DNA fibers, corresponding to the orientations defined in Fig. 2 (XX, YY, XY, and YX), are shown in Figs. 3, 4, 5, and 6. The observed spectral intensity ratios I_{bb}/I_{cc} and I_{bb}/I_{bc} for selected Raman bands of A and B DNA are listed in Tables 2 and 3. We next consider the polarization properties of some of the more prominent Raman bands of the A and B conformers of DNA.

I_{bb} and I_{cc} spectra: base vibrations of the 1100–1700 cm^{-1} region

Raman bands originating from in-plane CC and CN bond stretching vibrations of the base residues are expected to dominate the 1100–1700 cm^{-1} spectral interval (Lord and Thomas, 1967; Hartman et al., 1973). Normal coordinate calculations suggest that many of the modes involve 180° phase differences in the stretching of adjacent bonds of the heterocycles (Tsuboi et al., 1973). For both A and B DNA fibers, seven strong Raman bands are detected in this region of the Raman spectrum. In the I_{bb} spectrum of the B DNA fiber (Fig. 5, top), the peaks are centered at approximately 1257, 1303, 1339, 1375, 1487, 1578, and 1669 cm^{-1}; the corresponding bands of A DNA (Fig. 3, top) occur at 1257, 1304, 1339, 1376, 1486, 1577, and 1677 cm^{-1}. In B DNA, the band near 1339 cm^{-1}, due mainly to adenine, is less intense than the thymine band near 1376 cm^{-1}. The relative intensities of these adenine and thymine markers are reversed in A DNA. A similar reversal of intensity ratios has been observed in unpolarized Raman spectra of A and B fibers of calf thymus DNA (Prescott et al., 1984) and A and B fibers of poly(dA-dT)·poly(dA-dT) (Thomas and Benevides, 1985; Katahira et al., 1986). Additionally, Figs. 3 and 5 show that
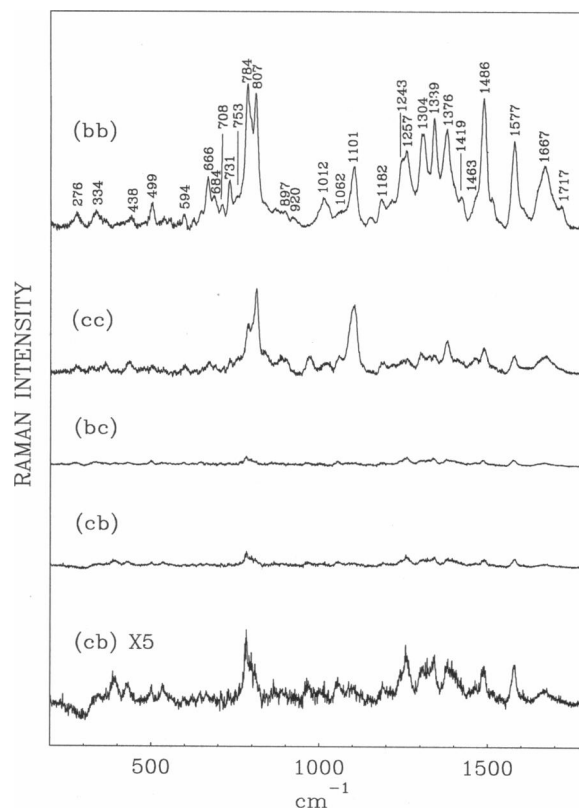

FIGURE 3 Raman spectra (I_{bb}, I_{cc}, I_{bc}, and I_{cb}) of an A DNA fiber corresponding to four tensor components (bb, cc, bc, and cb, respectively). The spectra were obtained with 514.5 nm excitation (λ_0) on a Jobin-Yvon S3000 spectrometer with Olympus BH2 microscope attachment. Sample temperature ($t = 10°C$) and relative humidity (RH = 75%) were maintained as described in the text. Each spectrum represents the average of six exposures of 2 min duration. Similar data were obtained with $\lambda_0 = 488.0$ nm.

all of the strong I_{bb} Raman bands noted above are greatly reduced in intensity in I_{cc} spectra of both A DNA and B DNA. This fact may be taken as an indication that, for each of the corresponding normal modes of vibration, the out-of-plane Raman tensor component (α_{zz}) is much smaller than at least one of the in-plane tensor components (α_{xx} or α_{yy}).

Although in both A and B fibers the base planes are oriented close to the normal to the fiber axis (c axis), the range of base tilt angles in A DNA ($\approx$10° to 20°) is somewhat greater than that in B DNA ($\approx$−6° to +2°). Accordingly, it might be anticipated that Raman anisotropies for the above-noted in-plane base vibrations, as measured by the polarized Raman intensity ratio I_{bb}/I_{cc}, should be greater for B DNA than for A DNA. However, Tables 2 and 3 indicate that this is not the case for any of the bands in question. Possible explanations are the following: (1) Raman tensors in the two conformers are intrinsically inequivalent; (2) geometric factors other than tilting of the hypothetical plane of the base pairs determine the different anisotropies of the two DNA conformations; (3) the B form fiber has lower crystallinity and consequently lesser order than the A form fiber, and this is a contributing factor to the different anisotropies. Further discussion of these points is given in the Summary and Conclusion section, below.
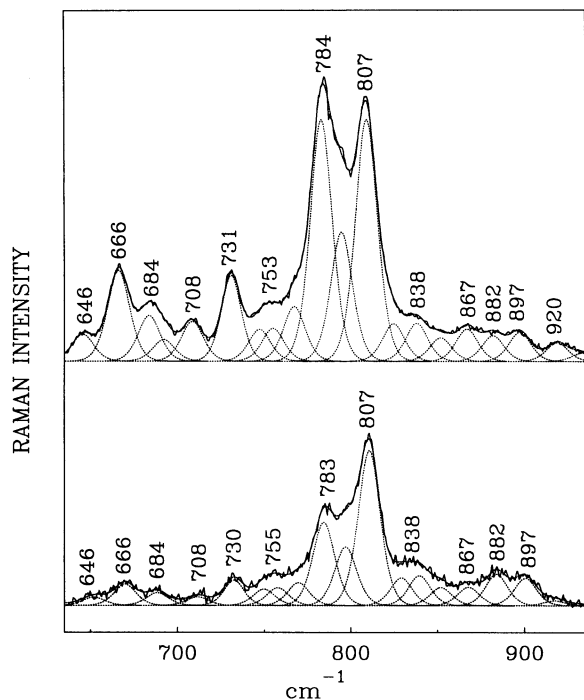
FIGURE 4 Curve decomposition of Raman bandshapes in the 650–920 cm^{-1} interval for I_{bb} and I_{cc} spectra of an A DNA fiber. Each spectrum is fitted to the minimum number (19 ± 1) of Gauss-Lorentz components required to accurately reproduce the experimentally observed bandshape. Experimental data are from Fig. 3.

I_{bb} and I_{cc} spectra: backbone vibrations of the 750–1100 cm^{-1} region

The I_{cc} spectrum of A DNA reveals a very strong Raman band at 807 cm^{-1} (Fig. 3, second spectrum from the top). B DNA exhibits instead a much weaker band at 836 cm^{-1} (Fig. 5, second from top). The 807 and 836 cm^{-1} frequencies correspond to well characterized "marker" bands of DNA, which are considered diagnostic of A and B conformations, respectively (Erfurth et al., 1972; Prescott et al., 1984; Thomas and Tsuboi, 1993). Extensive study of nucleic acid model compounds (Shimanouchi et al., 1964; Thomas et al., 1986) and normal coordinate analyses of isotopically labeled derivatives (Brown and Peticolas, 1975; Guan et al., 1994) suggest that these modes originate from vibrations associated with the 3′,5′-phosphodiester network (C—O—P—O—C). The normal modes in question are also considered to involve internal coordinates of the attached furanose moieties (Thomas et al., 1986; Toyama et al., 1993).

For B DNA, an additional marker band near 792 cm^{-1} has been proposed on the basis of deuteration effects observed in fibers of calf thymus DNA (Prescott et al., 1984) and poly(dA-dT)·poly(dA-dT) (Thomas and Benevides, 1985). A putative B backbone marker near 790 cm^{-1} would normally be masked in DNA of mixed base composition due to the presence of an overlapping Raman band near 784 cm^{-1} assignable to a ring mode of the cytosine residue (Lord and Thomas, 1967). The present results provide independent evidence of the B marker near 790 cm^{-1}. We see, e.g., from the
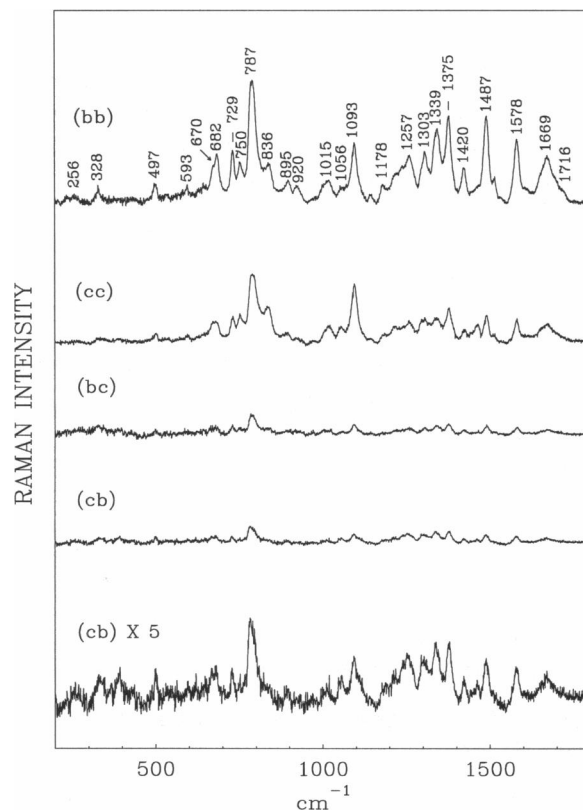

FIGURE 5 Raman spectra (I_{bb}, I_{cc}, I_{bc}, and I_{cb}) of a B DNA fiber corresponding to four tensor components (bb, cc, bc, and cb, respectively). Conditions: $\lambda_0 = 514.5$ nm, $t = 10°C$, RH = 92%. Other conditions are as given in Fig. 3. Similar data were obtained with $\lambda_0 = 488.0$ nm.

I_{bb} and I_{cc} spectra of A DNA (Fig. 3), that the out-of-plane Raman tensor component (α_{zz}) of the 784 cm^{-1} cytosine mode is relatively small. Accordingly, the strong band in the I_{cc} spectrum of B DNA cannot be assigned to this cytosine mode. A reasonable assignment is to a phosphorus-oxygen single bond stretching vibration, which is expected in this 750–850 cm^{-1} interval (Shimanouchi et al., 1964; Guan et al., 1994).

Fig. 7 compares the frequencies and intensities of Raman bands assigned to phosphodiester linkages in A DNA, B DNA, and dimethyl phosphate anion. The intensities of the respective 807, 792, and 759 cm^{-1} bands of these structures are comparable. It is therefore reasonable to assign these bands analogously, i.e., to a mode in each structure involving a large component of symmetrical stretching of phosphodiester linkages. With respect to the weaker 836 cm^{-1} band of B DNA, the question arises as to its assignment. One possibility is a mode related to antisymmetrical phosphodiester stretching (Shimanouchi et al., 1964; Prescott et al., 1984; Guan et al., 1994). The very weak counterpart at 816 cm^{-1} in dimethyl phosphate, and the apparent absence of a similarly weak band in A DNA could be explained by the fact that the C—O—P—O—C network has pseudo-C2 symmetry in these structures, but not in B DNA.

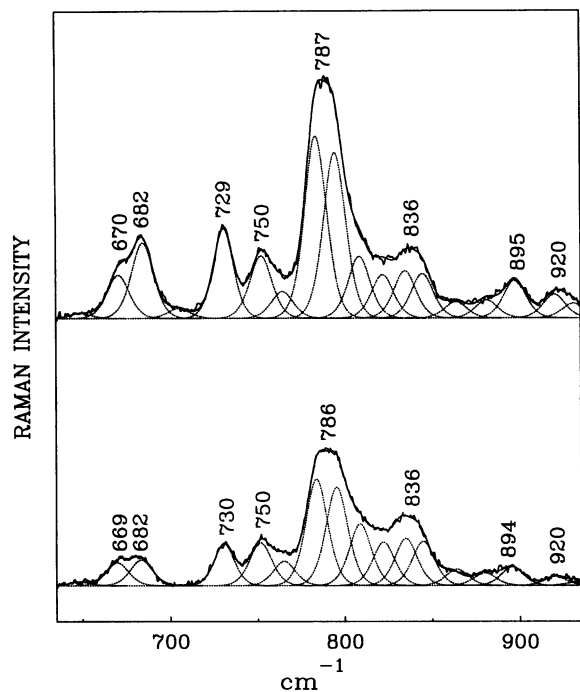The two relatively weak bands of B DNA at 895 and 920 cm^{-1} are assigned to bond stretching vibrations of the

FIGURE 6   Curve decomposition of Raman bandshapes in the 650–920 cm^{-1} interval for I_{bb} and I_{cc} spectra of a B DNA fiber. Each spectrum is fitted to the minimum number (17 ± 1) of Gauss-Lorentz components required to accurately reproduce the experimentally observed bandshape. Experimental data are from Fig. 5.

TABLE 2   Polarized Raman Intensity ratios of A DNA*

Band (cm^{-1})	Assignment	I_{bb}/I_{cc}	I_{bb}/I_{bc}
1667	C=O stretch (T)	4.5 ± 0.5	25 ± 5
1577	Ring mode (A, G)	5.8 ± 0.2	13 ± 1
1486	Ring mode (G, A)	6.7 ± 0.3	25 ± 2
1463	5'CH₂ scissor	<1	
1419	2'CH₂ scissor	4 ± 1	8 ± 1
1339	Ring mode (A, G)	7 ± 2	15 ± 1
1257	Ring mode (C, T)	5.8 ± 0.8	7 ± 1
1101	PO₂⁻ symmetric stretch	0.93 ± 0.05	>30
897	Deoxyribose ring	1.09 ± 0.05	>5
882	Deoxyribose ring	0.83 ± 0.05	>5
807	O-P-O stretch	1.57 ± 0.02	26 ± 4
784	Ring breathing (C)	2.9 ± 0.1	12 ± 5
753	Ring breathing (T)	2 ± 1	>10
731	Ring breathing (A)	3.4 ± 0.1	18 ± 5
666	Ring breathing (G)	4.3 ± 0.2	20 ± 5
499	PO₂⁻ scissor	3 ± 1	8 ± 1

*Experimental anisotropies, I_{bb}/I_{cc} and I_{bb}/I_{bc}, are from spectra of Figs. 3 and 4. An underlying weak component from B DNA may contribute to the bands at 1577, 1486, and 784 cm^{-1}, as discussed in the text.

deoxyribose ring. This assignment is supported by the observation that similar bands, at 852 and 898 cm^{-1}, in the Raman spectrum of thymidine are shifted by 12 and 17 cm^{-1}, respectively, upon ^{13}C substitution of C1', C2', C3', C4' and C5' positions of the deoxyribose residue (Tsuboi et al., 1994). Further support is provided by significant shifts of bands of guanosine in the 850–1000 cm^{-1} region upon deuterium substitution of the C1' proton (Toyama et al., 1993). Similarly weak bands are observed in A DNA at 882 and 897 cm^{-1} and in Z DNA at 868 and 902 cm^{-1} (Benevides et al.,

TABLE 3   Polarized Raman intensity ratios of B DNA*

Band (cm^{-1})	Assignment	I_{bb}/I_{cc}	I_{bb}/I_{bc}
1669	C=O stretch (T)	3.1 ± 0.2	11 ± 2
1578	Ring mode (A, G)	3.0 ± 0.2	10 ± 1
1487	Ring mode (G, A)	3.3 ± 0.2	11 ± 1
1465	5'CH₂ scissor	<1	
1420	2'CH₂ scissor	2.8 ± 0.3	7 ± 1
1339	Ring mode (A, G)	5.0 ± 0.4	6 ± 1
1257	Ring mode (C, T)	3.0 ± 0.4	5 ± 1
1093	PO₂⁻ symmetrical stretch	1.0 ± 0.1	6.7 ± 0.5
920	Deoxyribose ring	2.6 ± 0.5	6 ± 2
895	Deoxyribose ring	2.0 ± 0.5	4 ± 2
836	O-P-O stretch	0.95 ± 0.05	15 ± 5
792	O-P-O stretch	1.7 ± 0.2	7 ± 2
784	Ring breathing (C)	1.7 ± 0.2	7 ± 2
750	Ring breathing (T)	1.4 ± 0.2	10 ± 3
729	Ring breathing (A)	2.1 ± 0.2	7 ± 2
682	Ring breathing (G)	2.9 ± 0.3	5 ± 2
497	PO₂⁻ scissor	2.6 ± 0.5	3 ± 1

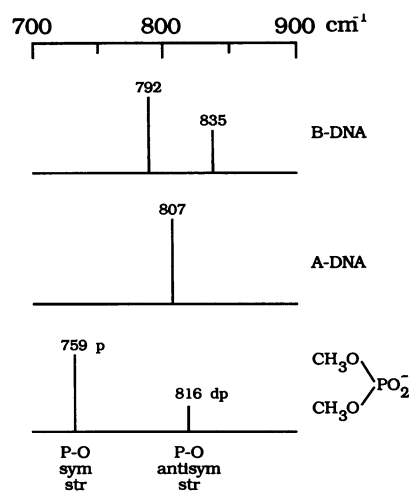*Experimental anisotropies, I_{bb}/I_{cc} and I_{bb}/I_{bc}, are from spectra of Figs. 5 and 6.

FIGURE 7   Frequencies and intensities of Raman bands in the region 700–900 cm^{-1} assignable to phosphorus-oxygen stretching vibrations of the phosphodiester groups in B DNA, A DNA, and dimethylphosphate anion. Abbreviations: p = polarized, dp = depolarized, ν_{sym} = symmetrical stretching frequency, $\nu_{antisym}$ = antisymmetrical stretching frequency. (See also Guan et al., 1994).

1993). We observe $I_{bb} < I_{cc}$ for the band of A DNA at 882 cm^{-1} as is also the case for the Z DNA band at 868 cm^{-1} (Benevides et al., 1993). For all other deoxyribose bands in this region, we find $I_{bb} > I_{cc}$.

The Raman band assigned to the symmetrical O⋯P⋯O stretching vibration of the nucleic acid phosphodioxy (PO₂⁻) group is expected near 1093 cm^{-1} in structures of the B form and near 1100 cm^{-1} in structures of the A form (Tsuboi, 1957; Sutherland and Tsuboi, 1957; Thomas, 1970; Erfurth et al., 1972; Prescott et al., 1984). We observe the PO₂⁻ markers at the expected frequencies in both A (Fig. 3) and B fibers (Fig. 5). For both DNA conformations, we note also that the I_{bb} and I_{cc} intensities are nearly equal. This contrasts sharply with results from polarized infrared spectroscopy, where $I_{\parallel} > I_{\perp}$ for A DNA, but $I_{\parallel} < I_{\perp}$ for B DNA (Pilet and Brahms, 1972; Nishimura et al., 1974). (Here, $I_{\parallel}$ and $I_{\perp}$ are the infrared

absorption intensities when the electric vector of the radiation is, respectively, parallel and perpendicular to the DNA fiber axis.) The fact that $I_{bb} \approx I_{cc}$ for the Raman PO_2^- mode can therefore be attributed to an intrinsically isotropic local Raman tensor.

The antisymmetrical O⋯P⋯O stretching vibration of the phosphodioxy group is expected near 1200 cm^{-1}. Although this vibration generates intense infrared absorption, the Raman scattering is characteristically very weak (Tsuboi, 1957; Shimanouchi et al., 1964; Thomas, 1970; Prescott et al., 1984). In the present study, no band definitively assignable to the antisymmetrical O⋯P⋯O mode could be detected in spectra of either the A or B DNA fiber.

I_{bb} and I_{cc} spectra:
base vibrations of the 600–800 cm^{-1} region

Relatively intense Raman bands assignable to ring breathing type motions of guanine, adenine, thymine, and cytosine are observed, respectively, at 666, 731, 753, and 784 cm^{-1} in A DNA and at 682, 729, 750, and 787 cm^{-1} in B DNA. As noted above, the 787 cm^{-1} band of B DNA actually represents the unresolved center of two overlapping bands due to cytosine (near 784 cm^{-1}) and the B backbone (near 790 cm^{-1}). For all of the ring modes $I_{bb} > I_{cc}$, which is consistent with the fact that the out-of-plane tensor component (α_{zz}) is smaller than in-plane components (α_{xx} and α_{yy}) (Benevides et al., 1993). As before, the Raman anisotropies for the in-plane base modes are greater in A DNA (Table 2) than in B DNA (Table 3).

I_{bb} and I_{cc} spectra:
backbone vibrations below 500 cm^{-1}

In both A and B fibers, the presently observed Raman band near 498 cm^{-1} corresponds to the similar Raman frequency reported previously for A, B, and Z nucleic acids (Prescott et al., 1984; Benevides et al., 1993). Assignment of this band to a valence angle bending mode (scissoring) of the phosphodioxy group is supported by normal coordinate analysis (Guan et al., 1994). High Raman anisotropy ($I_{bb} > I_{cc}$) distinguishes this phosphate group bending vibration from the previously discussed phosphorus-oxygen bond stretching modes occurring in the 750–1100 cm^{-1} interval (see section on backbone vibrations of the 750–1100 cm^{-1} region, above).

I_{bc} and I_{cb} spectra

All Raman bands in the I_{bc} and I_{cb} spectra (Figs. 3 and 5) are weak and therefore their signal-to-noise ratios are low. Nevertheless, some interesting conclusions can be drawn from these observations. First, the results show that $I_{bc} = I_{cb}$ for a given DNA fiber, i.e., the Raman spectrum of a fiber oriented along the c axis is invariant to an orthogonal interchange of the polarization directions of incident and scattered light. This is consistent with precise optical alignment of the Raman microscope and spectrometer system, with the absence of polarization artifacts, and with a relatively high de-

gree of unidirectional orientation of DNA along the fiber axis. Second, comparisons between A and B DNA indicate important tensor similarities and differences. For example, the bands near 1487, 1578, and 1669 cm^{-1} exhibit nearly equal intensities and band shapes in A and B fibers. On the other hand, the CH_2 scissoring mode, near 1420 cm^{-1}, gives a sharp band in B DNA but a more diffuse band in A DNA. The bands at 1303, 1339, and 1375 cm^{-1} are prominent only in B DNA, whereas the 1257 cm^{-1} band is prominent only in A DNA. Finally, of particular interest is the observation that the PO_2^- symmetrical stretching band appears much more prominently in the I_{bc} (or I_{cb}) spectrum of the B fiber than in that of the A fiber. Thus, the different orientations of phosphodioxy groups of A and B DNA, while silent in the I_{bb}/I_{cc} ratio, are clearly revealed in the I_{bb}/I_{bc} anisotropy.

Raman depolarization ratios of isotropic B DNA in solution

Table 4 lists the Raman depolarization ratios (ρ) for B DNA as determined from spectra of an aqueous solution of randomly oriented (isotropic) calf thymus DNA. Previously determined Raman depolarization ratios of aqueous mononucleotides (Ueda et al., 1993) are included in Table 4 for comparison. These data are interpretable as follows.

The 1670 cm^{-1} band is assignable to exocyclic carbonyl bond (C=O) stretching vibrations in the bases (Lord and Thomas, 1967). Among the three base residues containing the carbonyl function, the thymine contribution to the band intensity is large, that of guanine is small, and that of cytosine is negligible. The depolarization ratio ($\rho = 0.26$) observed for the 1670 cm^{-1} band of isotropic B DNA can be explained as a weighted average of the ρ values of the contributing base residues, in accordance with their respective intensities.

The 1578 cm^{-1} band of DNA comprises overlapping contributions from adenine and guanine (Lord and Thomas, 1967). The adenine contributor is almost completely depolarized ($\rho = 0.64$), whereas that of guanine is significantly polarized ($\rho = 0.34$) (Ueda et al., 1993, 1994). The intermediate value of ρ (0.54) observed for the 1578 cm^{-1} band of B DNA is thus consistent with values observed for purine mononucleotides. The 1489 cm^{-1} band of B DNA, also a composite of contributions from the two purines, is very strongly polarized in the nucleic acid ($\rho = 0.17$), as well as in the mononucleotides ($\rho = 0.11$ in GMP and 0.13 in dAMP); however, in this case the purine mononucleotide depolarizations are apparently not simply additive. Interestingly, the depolarization characteristics of the two purine ring modes at 1578 and 1489 cm^{-1} in isotropic DNA are dissimilar. This leads in turn to very different Raman tensor relationships for the two vibrational modes, as will be shown below.

Depolarization ratios of CH_2 scissoring modes near 1420 cm^{-1} have been examined in Raman spectra of both mononucleotides (Ueda et al., 1993) and oligonucleotide duplexes (Benevides et al., 1993). In every case the value of ρ is near 0.4. The present results show that this is also the case for isotropic B DNA.

TABLE 4　Raman depolarization ratios of isotropic B DNA and related nucleotides

Band (cm⁻¹)	Principal assignment	Depolarization ratio (ρ)				
		B DNA	dAMP	rGMP	rCMP	dTMP
1670	C=O stretch (T)	0.26 ± 0.05		0.40	0.12	0.172
1578	Ring mode (A, G)	0.54 ± 0.05	0.64	0.34		
1489	Ring mode (G, A)	0.17 ± 0.02	0.13	0.113		
1420	2'CH₂ scissor	0.42 ± 0.02	0.38			0.48
1375	Ring mode (T)	0.27 ± 0.03	0.20	0.19	0.2	0.382
1340	Ring mode (G, A)	0.43 ± 0.02	0.27	0.30		
1302	Ring mode (A, C)	0.33 ± 0.05	0.33		0.25	
1254	Ring mode (C, T)	0.47 ± 0.05			0.25	0.30
1092	PO₂⁻ sym stretch	<0.04*				
923	Deoxyribose	0.11 ± 0.05	0.2			0.1
900	Deoxyribose	0.36 ± 0.05	0.2			0.1
832	O-P-O stretch	0.17 ± 0.10‡				
792	O-P-O stretch	0.13 ± 0.05§				
782	Ring breathing (C)	0.17 ± 0.05			0.064	
749	Ring breathing (T)	0.10 ± 0.05				0.07
728	Ring breathing (A)	0.13 ± 0.05	0.09			
683	Ring breathing (G)	0.19 ± 0.05		0.11		
670	Ring mode (T)	0.18 ± 0.05				0.30
497	PO₂⁻ scissor	0.15 ± 0.10¶				

*For the 1085 cm⁻¹ band of dimethyl phosphate, ρ = 0.06 (Guan et al., 1994).
‡ For the 827 cm⁻¹ band of dimethyl phosphate, ρ = 0.56 (Guan et al., 1994).
§ For the 754 cm⁻¹ band of dimethyl phosphate, ρ = 0.03 (Guan et al., 1994).
¶ For the 503 cm⁻¹ band of dimethyl phosphate, ρ = 0.48 (Guan et al., 1994).

The four intense Raman bands of B DNA at 1254, 1302, 1340, and 1375 cm⁻¹ (Table 4) are assignable to in-plane ring vibrations of the base residues, as noted in the section on base vibrations of the 1100–1700 cm⁻¹ region. A common characteristic of each of these Raman bands in isotropic B DNA is a depolarization ratio of intermediate magnitude ($0.25 < \rho < 0.50$). In accordance with Fig. 1, such a ρ value is indicative of a relatively anisotropic Raman tensor ($|r_1|, |r_2| > 1$). Accordingly, these bands are potentially good candidates for probing DNA base orientations in complex biological assemblies by polarized Raman spectroscopy.

The PO₂⁻ symmetrical stretching band at 1092 cm⁻¹ is very highly polarized ($\rho < 0.04$). Hence, from Fig. 1 we expect $r_1 \approx r_2 \approx 1$, and the Raman tensor should be relatively spherical or isotropic, i.e., $\alpha_{xx} \approx \alpha_{yy} \approx \alpha_{zz}$. Accordingly, the 1092 cm⁻¹ band in polarized Raman spectra is not expected to be a useful indicator of residue orientation.

In accordance with the assignments proposed above for the bands at 895 and 920 cm⁻¹ in the B DNA fiber, we suggest assignment of the 900 and 923 cm⁻¹ bands in the B DNA solution to bond stretching vibrations of the deoxyribose ring. Because of its higher Raman polarization (ρ = 0.11), the 923 cm⁻¹ band is considered to represent a more symmetrical furanose ring stretching vibration than does the 900 cm⁻¹ band (ρ = 0.36). These assignments are consistent with those proposed previously for the sugar group of thymidine (Tsuboi et al., 1994).

Depolarization ratios for phosphodiester modes of the 750–850 cm⁻¹ interval could not be determined accurately from the spectra because of significant overlap with intense bands of the base residues. To estimate the depolarization ratios, the complex bandshape was subjected to curve fitting to the minimum number of Gauss-Lorentz components con-

sistent with the experimental data. The results in Table 4 indicate that the bands at 792 cm⁻¹ (ρ = 0.13) and 832 cm⁻¹ (ρ = 0.17) are both highly polarized. In B DNA, therefore, the depolarization ratios suggest that a distinction between symmetrical and antisymmetrical stretching motions of the C—O—P—O—C network is inappropriate.

It is interesting to note that of the bands assigned to ring-breathing type motions of the base residues [683 (G), 728 (A), 749 (T), and 782 cm⁻¹ (C)], those of G and C exhibit significantly higher ρ values, i.e., lower polarizations, in B DNA than in the corresponding mononucleotide. This may result from Raman tensor perturbations specific to pairing and stacking of these base residues in B DNA.

Raman tensors for local vibrations of DNA

Intensity ratios I_{bb}/I_{cc} and I_{bb}/I_{bc} as a function of r_1 and r_2

Here we determine the most probable shape of the local Raman tensor associated with each Raman band of DNA. Specifically, we seek to identify for each Raman tensor the directions of its principal axes x, y, and z with respect to the local atomic framework (X, Y, Z), and the relative magnitudes of the tensor quotients, r_1 and r_2, defined in Eq. 1, above. For this purpose, we require the experimental intensity ratios, I_{bb}/I_{cc} and I_{bb}/I_{bc}, obtained from the polarized Raman spectrum of oriented DNA (Figs. 3–6), as well as the experimental depolarization ratios, $\rho = I_{\perp}/I_{\parallel}$, obtained from perpendicular and parallel components of the Raman spectrum of unoriented (isotropic) DNA (Table 4).

Because the Raman tensor calculation is underdetermined by the available data, an iterative methodology is employed. We select a trial set of principal axes for each molecular subgroup and calculate tensor quotients consistent with the

experimental data. The process is repeated for additional trial axes until an optimum fit between calculated and experimental data is reached. Typical trial sets of principal axes are defined and illustrated in Table 5 and Fig. 8.

Further details of the procedure are as follows. Each tensor coordinate system (x, y, z) is defined by its direction relative to three nonlinearly arranged atoms of the molecular subgroup, designated as atoms A, E1 and E2, as shown in Table 5. Thus, y is parallel to the line connecting E1 and E2; x is perpendicular to y and intersecting A, and z is perpendicular to the xy plane. For the specified tensor coordinate system, the nine direction cosines of Eq. 3, a–f are calculated on the basis of the atomic coordinates of A, E1, and E2 (Langridge et al., 1960; Fuller et al., 1965; Arnott and Hukins, 1972). By use of the calculated direction cosines and the set of atomic coordinates for A, E1, and E2, as well as given values for r_1 and r_2 (consistent with ρ, Eq. 2), we can obtain by Eq. 3, a–f the tensor quotients α_{XX}/α_{ZZ}, α_{YY}/α_{ZZ}, ..., α_{ZX}/α_{ZZ}. From these data we calculate the corresponding intensity ratios, I_{bb}/I_{cc} and I_{bb}/I_{bc}. The calculated results provide a contour map of theoretical anisotropies in $[r_1, r_2]$ space for each trial coordinate system. Examples of such calculations are presented in Figs. 9 and 10.

A survey of the A DNA contour maps in Fig. 9 indicates, not surprisingly, that they are highly dependent on the choice of atomic coordinates. In the structure of Fuller et al. (1965), e.g., the tilt of the normal to the purine plane away from the c axis is achieved by rotation of the base about its C4—C5 bond, whereas in the structure of Arnott and Hukins (1972) this tilt is with respect to the C4—N7 line. Accordingly, the contour maps for G1 and G3 are similar for the former structure but greatly different for the latter (Fig. 9, top maps). Also, for G2, with the coordinates of Arnott and Hukins, the map is symmetrical to interchange of r_1 and r_2, a consequence of the fact that in this structure the x and y axes are tilted equally from the c axis; this is not the case for the A DNA structure of Fuller et al. (1965). On the other hand, in both B DNA models, all base planes are nearly perpendicular to

TABLE 5   Principal axes for localized vibrational modes of DNA

DNA residue	Coordinate system*	Reference atoms		
		A	E1	E2
Purine base	G1	N3	N1	N9
	G2	N3	N1	N7
	G3	N3	C2	N7
Pyrimidine base	C1	N1	N3	C5
	C2	N1	C2	C5
	C3	N1	C2	C4
2' Methylene	2'CH$_2$	C2'	C1'	C3'‡
5' Methylene	5'CH$_2$	C5'	O5'	C4'‡
Phosphate	P1	P	O$^-$	O$^-$
Deoxyribose	D1	O4'	C2'	C3'

*See Fig. 8 and text.
‡An alternate coordinate system for the methylene group involves interchange of the tensor axes y and z, which is equivalent to replacing r_1 by r_1/r_2 and r_2 by $1/r_2$, so that x is along the <HCH bisector and y is along the line connecting the two H atoms.

c. Therefore, the calculated maps (Fig. 10) are nearly equivalent for the three axial choices of a purine (G1, G2, G3) or pyrimidine (C1, C2, C3). Consequently, for B DNA, we cannot distinguish among the various choices of tensor axes on the basis of the polarized Raman spectra.

Parametric determination of r_1 and r_2

For each Raman band, plausible sets of tensor quotients (r_1 and r_2 values) were obtained as the points of intersection in $[r_1, r_2]$ space of the measured I_{bb}/I_{cc} anisotropy (Fig. 9 or 10) and depolarization (Fig. 1) contour maps. For example, in the case of the 1667 cm^{-1} Raman band of A DNA, 12 $[r_1, r_2]$ pairs are consistent with the experimental I_{bb}/I_{cc} ($= 4.5$) and ρ ($= 0.26$) values, six for each of the proposed thymine atomic coordinates. The 12 candidate pairs are listed in the upper part of Table 6. We include in the last column of Table 6 the expected I_{bb}/I_{bc} anisotropy for each $[r_1, r_2]$ pair. Interestingly, these differ greatly from one another and allow us to narrow the number of candidates to those consistent with the measured I_{bb}/I_{bc} value of 25 ± 5 for A DNA. Thus, the available experimental data on A DNA restrict the 1667 cm^{-1} Raman tensor to either of the following $[r_1, r_2]$ pairs: [3.7, −0.3] or [−0.2, 4.2].

Another 12 $[r_1, r_2]$ possibilities exist for the 1669 cm^{-1} band of B DNA. These are listed in the lower part of Table 6, each with its calculated I_{bb}/I_{bc} anisotropy. For B DNA, the observed value of I_{bb}/I_{bc} ($= 11 \pm 2$) is substantially less than all calculated values ($65 \le I_{bb}/I_{bc} \le 439$). Thus, no single $[r_1, r_2]$ pair satisfactorily explains both the A and B DNA data. The discrepancy between measured and calculated I_{bb}/I_{bc} anisotropies of B DNA is most likely due to either incomplete unidirectional orientation of the B form fiber or to displacements of the base planes from strict planarity (e.g., propeller twist), or to a combination of such effects. On the other hand, we cannot rule out the possibility that dissimilarity between local Raman tensors of the 1667 cm^{-1} band of A DNA and the 1669 cm^{-1} band of B DNA is due to intrinsic differences in the normal modes associated with the two DNA structures.

To simplify the following treatment, we restrict further analysis to the A and B DNA coordinates of Arnott and Hukins (1972). These choices, though somewhat arbitrary, are consistent with previous work.

Shapes of specific DNA Raman tensors

Table 7 gives $[r_1, r_2]$ pairs determined for each prominent Raman band of DNA using the iterative, parametric approach outlined above and the indicated coordinate systems for A and B DNA. The relatively small uncertainties for several Raman tensors of A DNA reflect the apparently high crystallinity and order achieved for the A form fiber. On the other hand, the Raman tensors listed in Table 7 for B DNA are semiquantitative, given the apparently greater degree of structural heterogeneity in the B form fiber. These B form

FIGURE 8 Principal axes $(x, y,$ and $z)$ of the local Raman tensors representing selected base, sugar, and phosphate group vibrations of DNA, as described in the text and Tables 5–7. The coordinate systems are designated G1, G2, and G3 for purine base vibrations, C1, C2, and C3 for pyrimidine base vibrations, $2'CH_2$ and $5'CH_2$ for CH_2 scissoring vibrations, P1 for phosphodioxy and phosphodiester vibrations, and D1 for deoxyribose ring vibrations. Within the limits of the present experimental data, these coordinate systems (or alternates involving only permutations of the principal axes) represent all reasonable choices for the Raman tensor calculations.
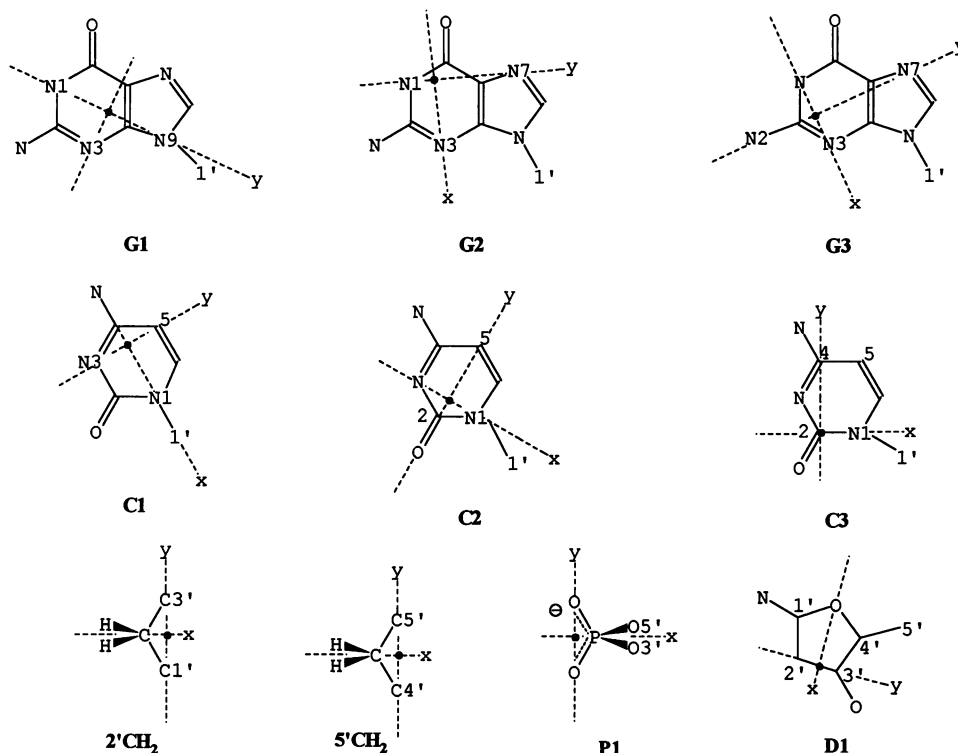

Raman tensors may be regarded as averaged over the distribution of helical orientations sampled by the laser beam. Nevertheless, Table 7 shows that most of the Raman tensors are not altered greatly by the $B \rightarrow A$ structure transition. We next consider the specific shapes of several of the DNA Raman tensors.

Carbonyl stretching: 1667 cm^{-1}: As noted above, the 1667 cm^{-1} band of A DNA is a composite assigned to C=O stretching vibrations of the base residues, among which thymine is the main contributor. By comparison, the guanine contribution is small,

and that from cytosine is negligible (Lord and Thomas, 1967; Ueda et al., 1993). In crystalline thymidine, Raman bands (with coordinate system and corresponding tensors) are observed at 1642 (C2, $r_1 = 2, r_2 = 5$) and 1665 cm^{-1} (C1, $r_1 = 4.35, r_2 = -3.9$), assignable to 2C=O and 4C=O groups, respectively (M. Tsuboi, T. Ueda, K. Ushizawa, and M. Saitoh, unpublished results). The Raman tensor of A DNA at 1667 cm^{-1} (Table 7) is well explained as the resultant of two overlapping Raman tensors from the thymine 2C=O and 4C=O groups.

FIGURE 9 Theoretical I_{bb}/I_{cc} values represented in r_1, r_2 space for A DNA, based upon the atomic coordinates of Fuller et al. (1965), left, and Arnott and Hukins (1972), right. Each map is labeled to indicate the tensor principal axes of Fig. 8 to which it corresponds. Each contour line defines the set of r_1, r_2 coordinates consistent with the indicated I_{bb}/I_{cc} value. (E.g., a guanine or adenine Raman band for which $I_{bb}/I_{cc} = 1$ and $r_1 = -5$ would be expected to exhibit either $r_2 = 2.5$ or $r_2 = 9$ in the G1 coordinate system. Note, however, that in the procedure described here, the candidate values for r_1 and r_2 are identified initially as points of intersection between the appropriate ρ contour of Fig. 1 (based upon the experimentally measured depolarization ratio) and the appropriate I_{bb}/I_{cc} contour in the assumed coordinate system (based upon the experimentally measured anisotropy).)

A-DNA
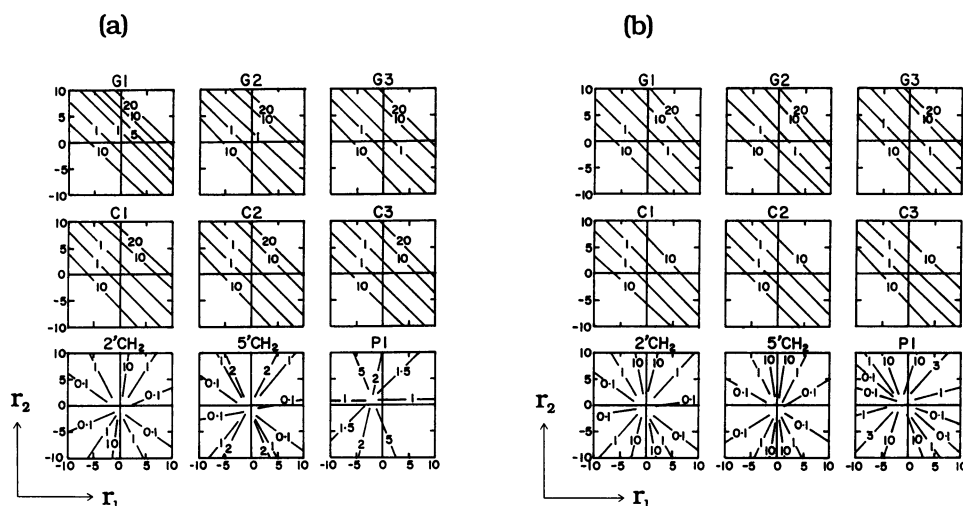
I_{bb} / I_{cc}

B-DNA

I_{bb} / I_{cc}

(a)

(b)
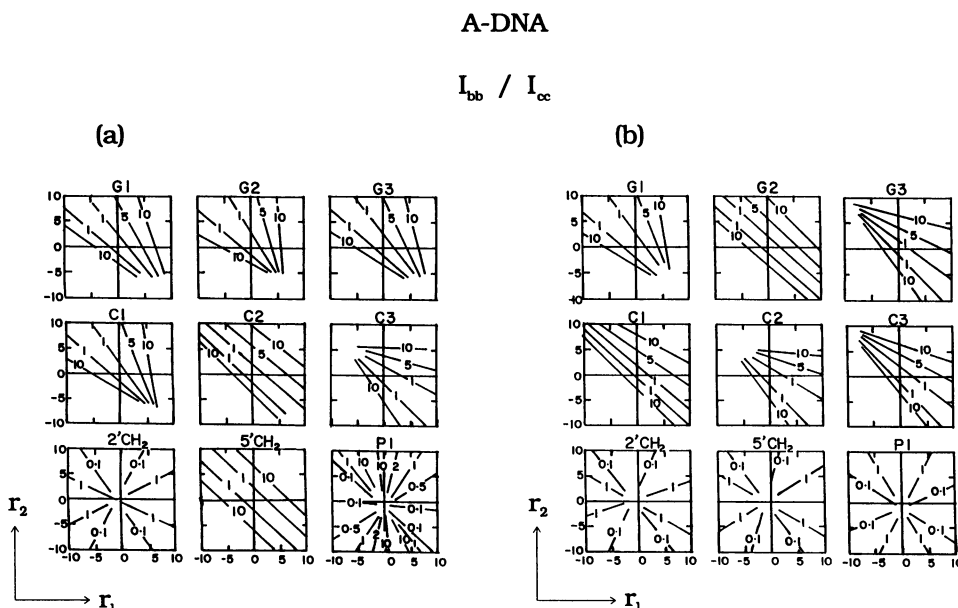
FIGURE 10 Theoretical I_{bb}/I_{cc} values represented in r_1,r_2 space for B DNA, based upon the atomic coordinates of Langridge et al. (1965), left, and Arnott and Hukins (1972), right. Other notation is defined in Fig. 9.

TABLE 6 Raman tensors and anisotropies for the 1667 cm^{-1} band

Structure	Coordinate system	r_1	r_2	I_{bb}/I_{bc}*
A DNA[‡]	C1	0.3	9.1	5.1
		3.7	−0.3	21.8
	C2	−0.2	5.6	10.0
		5.6	−0.1	8.6
	C3	−0.2	3.7	32.0
		9.1	0.4	4.8
A DNA[§]	C1	−0.2	5.3	10.6
		5.8	−0.1	9.6
	C2	−0.3	3.8	35.9
		8.3	0.1	5.2
	C3	−0.2	4.2	22.4
		7.2	0.0	6.4
B DNA[¶]	C1	−0.3	3.9	439
		3.9	−0.3	114
	C2	−0.3	3.9	185
		3.9	−0.3	177
	C3	−0.3	3.9	111
		3.8	−0.3	417
B DNA[§]	C1	−0.3	3.9	70
		3.8	−0.3	213
	C2	−0.3	3.9	118
		3.9	−0.3	98
	C3	−0.3	3.8	269
		4.0	−0.3	65

*For A and B DNA the experimental values of I_{bb}/I_{cc} are 4.5 and 3.1, respectively, and ρ is 0.26. These experimental values are reproduced using any of the tabulated sets of $[r_1,r_2]$ with the indicated coordinate system. Differences occur only for the calculated values of I_{bb}/I_{bc} listed in this column.

[‡]Atomic coordinates of Fuller et al., 1960.
[§]Atomic coordinates of Arnott & Hukins, 1972.
[¶]Atomic coordinates of Langridge et al., 1965.

Purine ring mode: 1577 cm^{-1}: The 1577 cm^{-1} band of DNA results from overlapping contributions from guanine and adenine residues. Since values of ρ are different for bands in mononucleotides of guanine (0.34) and adenine

(0.64), the corresponding Raman tensors are also expected to be different, as indeed has been confirmed for the mononucleotides (Ueda et al., 1993, 1994). The tensors determined for the corresponding band in either A or B DNA (Table 7) are intermediate in magnitude between the values determined for the purine mononucleotides (Ueda et al., 1993, 1994). The Raman tensor for this purine mode is one of the most interesting among all localized DNA base vibrations in the sense that r_1 and r_2 are of opposite signs. Thus, one of the in-plane components of polarizability change with vibration decreases when the other in-plane component increases, and vice versa.

Purine ring mode: 1486 cm^{-1}: Guanine is the major contributor to the purine-specific 1486 cm^{-1} band. The depolarization ratios are similar for guanine (0.11) and adenine (0.13) (Ueda et al., 1993), and therefore comparable in-plane tensor components (α_{xx},α_{yy}) are expected from both purines. In B DNA, $\rho = 0.17$ (Table 4), which is somewhat larger than observed for either purine. This may be due to an effect of secondary structure. The Raman tensor for the 1486 cm^{-1} band is found to be highly asymmetrical in shape, although the signs of all principal tensor components are the same (Table 7).

Methylene scissoring: 1419 and 1463 cm^{-1}: The Raman tensor for a CH_2 scissoring vibration, the frequency of which is anticipated within the 1400–1470 cm^{-1} interval, often has its greatest component along a line connecting the two hydrogens. On the basis of the A DNA model of Arnott and Hukins (1972), the H$\cdots$H line of the 5'CH_2 group is essentially parallel to the c axis, whereas the H$\cdots$H line of the 2'CH_2 group is not. Therefore, I_{cc} is expected to be much greater than I_{bb} for the Raman band assignable to 5'CH_2 scissoring. Of the two viable Raman frequencies in Fig. 3, only that at 1463 cm^{-1} has the expected anisotropy for 5'CH_2 and is so assigned, while the 1419 cm^{-1} band is assigned to 2'CH_2 scissoring. With this assignment scheme, a reasonable set of

TABLE 7 Shapes and orientations of Raman tensors of DNA

A DNA band	Axes	r_1	r_2	B DNA band	Axes	r_1	r_2
1667	C3	-0.2 ± 0.3	4.2 ± 0.3	1669	C3	-0.3	3.8
1577	G3	0.6 ± 0.2	-4.8 ± 0.4	1578	G3	0.5	-3.9
1486	G2	1.1 ± 0.3	6.0 ± 0.6	1487	G2	0.25	3.55
1419	2'CH₂	-0.35 ± 0.05	0.28 ± 0.02	1420	2'CH₂	-0.15	0.05
		-1.25 ± 0.25*	3.5 ± 0.3*			-3*	20*
1339	G3	-0.5 ± 0.3	-3.7 ± 0.6	1339	G3	-0.4	-3.9
1257	C3	-2.0 ± 0.4	5.8 ± 0.8	1257	C3	-2.0	5.6
1101	P1	1.0‡	0.9‡	1093	P1	1	1
897	D1	2 ± 1	5 ± 2				
807	P1			836	P1	9	3
784	C3	4.2 ± 0.6	0.5 ± 0.4	784	C3	2.6	0.1
753	C3	2.8 ± 1.0	0.7 ± 0.5	750	C3	2.2	0.2
731	G2	0.7 ± 0.4	3.6 ± 0.4	729	G2	0.35	2.6
666	G2	0.5 ± 0.2	4.5 ± 0.2	682	G2	0.2	3.3

*Values calculated for the alternate coordinate system of the methylene group. See Table 5 footnote.

‡Consistent with values of I_{bb}/I_{cc} and ρ observed in aqueous B DNA. However, the alternative $[r_1, r_2]$ pairs, [0.6, 0.1] and [3, 4.5], are also consistent with the experimental anisotropies (Table 2), as discussed in the text.

tensor quotients ($r_1 = -1.25$, $r_2 = 3.5$) is also obtained for the 2'CH₂ group (1419 cm⁻¹ band), consistent with observed values of I_{bb}/I_{cc} (= 4) and ρ (= 0.42). In further support of these assignments, we were unable to find a satisfactory set of tensors under the presumption that both the 5'CH₂ and 2'CH₂ scissoring modes contribute to the 1419 cm⁻¹ band.

Purine mode: 1339 cm⁻¹: The 1339 cm⁻¹ band of DNA is due primarily to an adenine ring vibration, although the band is partially overlapped on its low frequency side by a guanine ring mode occurring near 1322 cm⁻¹ in A DNA or 1319 cm⁻¹ in B DNA (Prescott et al., 1984). In the Z DNA crystal structure of d(CGCGCG), the corresponding guanine band occurs at 1318 cm⁻¹ and its Raman tensor has been determined (G3, $r_1 = -0.5$, $r_2 = 10.8$) (Benevides et al., 1993). Although a similar tensor (G3, $r_1 = -1.8$, $r_2 = 6.0$) for the 1339 cm⁻¹ adenine band of A DNA satisfactorily reproduces the observed values of I_{bb}/I_{cc} (= 7) and ρ (= 0.43), it is not consistent with the observed value of I_{bb}/I_{bc} (= 15). The only tensor consistent with all of the experimental data for the 1339 cm⁻¹ band is that given in Table 7 (G3, $r_1 = -0.5$, $r_2 = -3.7$). Since both r_1 and r_2 are negative, the sign of α_{zz} is opposite to that of both α_{xx} and α_{yy}.

Pyrimidine mode:1257 cm⁻¹: The 1257 cm⁻¹ band of A DNA is composed of thymine and cytosine contributions. The experimental data are reproduced satisfactorily by a tensor (C3, $r_1 = -2.0$, $r_2 = 5.8$), which is similar to that derived previously for the 1264 cm⁻¹ cytosine component (C2, $r_1 = -0.2$, $r_2 = 6.3$) of Z DNA (Benevides et al., 1993). Like the tensors for the 1577 cm⁻¹ purine mode (above), the tensors for the 1257 cm⁻¹ pyrimidine mode are not all of the same sign.

A DNA backbone modes: 499,807 and 1101 cm⁻¹: For the 1101 cm⁻¹ band, assigned to the PO₂⁻ symmetrical stretching vibration, we observe $I_{bb}/I_{cc} = 0.93 \pm 0.05$, which implies that the Raman tensor is nearly isotropic. In fact, this experimental intensity ratio can be closely approximated (calculated $I_{bb}/I_{cc} = 0.92$) if $r_1 = 1$ and $r_2 = 0.9$ in the P1 axis system, consistent with a nearly isotropic Raman tensor. However, this $[r_1,r_2]$ pair requires that $I_{bb} \gg I_{bc}$, i.e., I_{bc} must be vanishingly small. Our spectra (Fig. 3) suggest an ex-

perimental value for $I_{bb}/I_{bc} \approx 30$, in semiquantitative agreement with the calculated value.

As may be judged from the P1 contour plot shown for $I_{bb}/I_{cc} = 1$ in Fig. 9, not only the above $[r_1, r_2]$ pair, but also more anisotropic pairs, e.g. [0.6, 0.1] and [3, 4.5], provide reasonably good fits to the experimental data. These $[r_1, r_2]$ pairs have been included in Table 7 (‡). More definitive determination of the shape of this Raman tensor should be possible when more precise measurement of the I_{bc} spectrum becomes available.

Because of the probable isotropic shape of its Raman tensor (i.e., $r_1 \approx r_2 \approx 1$), the 1101 cm⁻¹ band is not recommended as a potential indicator of A DNA (or RNA) residue orientation in supramolecular assemblies, despite its intrinsically high Raman intensity. On the other hand, the isotropic nature of the band would favor its usefulness as an intensity standard in both polarized and unpolarized Raman studies.

The 807 cm⁻¹ band of A DNA, assigned to P—O single bond stretching, exhibits modest intensity anisotropy ($I_{bb}/I_{cc} = 1.57$). However, model compounds exhibiting this marker band in solution are not available, and accordingly its ρ value is not known. Therefore, detailed shape of the Raman tensor cannot be ascertained with present methods. Similarly, the lack of a reliable ρ value for the 499 cm⁻¹ band, assigned to PO₂⁻ scissoring, precludes present determination of its Raman tensor.

B DNA backbone modes: 792,835 and 1093 cm⁻¹: The 1093 cm⁻¹ band of B DNA, like its counterpart at 1101 cm⁻¹ in A DNA, is assigned unambiguously to the PO₂⁻ symmetrical stretching vibration. As also observed for the 1101 cm⁻¹ band (above), the 1093 cm⁻¹ band exhibits nearly equivalent I_{bb} and I_{cc} intensities, and a markedly smaller I_{bc} intensity (Table 3). Again the tensor shape is considered likely to be isotropic (Table 7), although the experimental I_{bc} value is not as small as expected. However, an isotropic Raman tensor for the 1093 cm⁻¹ band is consistent with the experimental evidence for a small depolarization ratio ($\rho < 0.04$, Table 4), and we propose this band as an appropriate intensity standard in polarized and unpolarized Raman spectra of B form nucleic acids.

If more precise determination of the I_{bc} intensity becomes feasible, e.g., through measurement of the polarized Raman

spectrum of an oriented single crystal of a *B* DNA oligo-nucleotide, it should be possible to establish with greater certainty the isotropic shape of this Raman tensor. Tentatively, we speculate that the unusually high I_{bc} value for the *B* conformer (1093 cm^{-1} band) may reflect a conformation-specific effect of solvent and/or cationic interactions with the negatively charged phosphate groups.

As noted above, the two phosphodiester related bands of *B* DNA at 792 and 835 cm^{-1} are also of interest. Although accurate ρ values could not be determined because of band overlap, it is clear from present data that neither has a ρ value as large as the value of 0.67 observed for the phosphodiester antisymmetric stretching vibration of dimethyl phosphate anion (Guan et al., 1994). Thus, the Raman tensors of the *B* DNA phosphodiester markers at 835 and 792 cm^{-1} must be greatly different from the similar frequencies (816 and 759 cm^{-1}) of dimethyl phosphate.

Furanose ring modes: 882 and 897 cm^{-1}: Lord and Thomas assigned a Raman band at 880 cm^{-1} in the Raman spectrum of D(−)-ribose to coupled C—O and C—C furanose-ring stretching on the basis of its insensitivity to deuteration of hydroxyl substituents and its consistent appearance in Raman spectra of all ribonucleosides and ribo-nucleotides (Lord and Thomas, 1967). Tsuboi and co-workers, in a recent polarized Raman study of crystalline thymidine (M. Tsuboi, T. Ueda, K. Ushizawa and M. Saitoh, unpublished results), established that the C3'-*endo* deoxyri-bose ring gives two Raman bands in the 850–920 cm^{-1} region, *viz.* at 853 (D1, $r_1 = 2.3$, $r_2 = 2.6$) and 899 cm^{-1} (D1, $r_1 = 1.3$, $r_2 = 1.1$), and assigned the latter to a furanose ring breathing vibration. The bands observed at 882 and 897 cm^{-1} in *A* DNA are assigned by analogy with those of the thy-midine crystal to C3'-*endo* deoxyribose rings. However, the I_{bb}/I_{cc} values observed for these two bands (Table 2), are not reproduced by the same tensor parameters determined for thymidine. For example, if we allow $r_1 = 1.3$ and $r_2 = 1.1$ for the 897 cm^{-1} band of *A* DNA, then $I_{bb}/I_{cc} = 0.72$; whereas Table 2 shows that the observed intensity ratio is 1.09. The Raman tensor determined here for the 897 cm^{-1} band of *A* DNA (Table 7) is far more anisotropic than its counterpart in thymidine. We attribute this to effects of the 3' and 5' phosphoryl substituents, which likely alter the nature of the normal mode in DNA.

Ring breathing modes: 666 (G), 731 (A), 753 (T) and 784 (C) cm^{-1}: Six-membered aromatic ring systems are expected to exhibit a prominent Raman band in the 600–1000 cm^{-1} interval associated with a quasisymmetrical ring stretching or "breathing" mode. In accordance with previous studies of nucleic acids and nucleotide model compounds (Lord and Thomas, 1967; Prescott et al., 1984), *A* DNA bands are so assigned at 666 (G), 731 (A), 753 (T) and 784 (C) cm^{-1}. The computed Raman tensors are given as the last four entries of Table 7. Interestingly, several characteristics are common to all of these Raman tensors. In each case: (1) r_1 and r_2 are both positive, which signifies that α_{xx}, α_{yy}, and α_{zz} all have the same sign. (2) The largest component of each Raman tensor (α_{xx}) is nearly parallel to the long axis of the base pair. (3) The intermediate tensor component (α_{zz}) is perpendicular to

the base plane. (4) The smallest tensor component (α_{yy}) is perpendicular to the long axis of the base pair. It seems likely that these tensor attributes are diagnostic of the purine or pyrimidine ring breathing mode. The tensor characteristics may therefore serve to identify such modes in polarized Raman spectra of oriented biological assemblies.

Nonlocal Raman tensors of the DNA helix for biological applications

Finally, we note that a frequent goal in biological applications of vibrational spectroscopy is the determination of specific residue orientations in ordered macromolecular assemblies. In the past this has been achieved primarily by means of infrared spectroscopy, through examination of the dichro-ism of a particular infrared absorption band. Infrared dichro-ism is mediated by a vector quantity, namely, the infrared transition dipole moment. In the Raman effect, the corresponding quantity required to assess residue orientation is a tensor rather than a vector, and its experimental determination is more challenging. In the present study we have determined local Raman tensors for DNA vibrations originating in specific atomic groups of the bases and backbone. In principle, these local Raman tensors may be exploited not only to determine orientations of the corresponding residues of helical DNA, but also to examine the orientation of the helix itself within a macromolecular assembly. To facilitate such determinations it is convenient to assign to each Raman band of DNA an effective helix (nonlocal) Raman tensor with principal components $\alpha_{x'x'}$, $\alpha_{y'y'}$, $\alpha_{z'z'}$, for which we define $r_{1'} = \alpha_{x'x'}/\alpha_{z'z'}$ and $r_{2'} = \alpha_{y'y'}/\alpha_{z'z'}$. Thus, an effective helix Raman tensor replaces each local Raman tensor of Eq. 1, a–b. This is equivalent to assuming that each localized vibration is replaced by a cooperative vibration involving the coupling of all identical residues in the macromolecule. (In practice, such coupling is very small.) As an example, consider the 1578 cm^{-1} band of *B* DNA. The nonlocal Raman tensor assignable to the 1578 cm^{-1} band would have the following shape. One principal axis (z') would be parallel to the helix axis, and the remaining two (x' and y') would be perpendicular to the helix. By virtue of symmetry, $\alpha_{x'x'} = \alpha_{y'y'}$, and $r_{1'} = r_{2'}$. Accordingly, from Eqs. 7 and 8 and Table 3, we have $(\alpha_{x'x'} + \alpha_{y'y'})^2/4\alpha_{z'z'}^2 = I_{bb}/I_{cc} = 3.0$. Therefore, $r_{1'} = r_{2'} = \pm1.73$. On the basis of the value of ρ observed for *B* DNA in solution (Table 4), the negative sign is preferred. By use of this result and the Raman anisotropy measured at 1578 cm^{-1} for an appropriately oriented biological assembly containing *B* DNA, it is possible to estimate the average tilt of the purine C2—N7 line from the direction of orientation, and accordingly, the angle of tilting of the *B* DNA helix axis. In Table 8 we have compiled the effective helix Raman tensors for several anisotropic bands of *B* and *A* DNA. We propose these as a starting point for application of the present results to native biological assemblies.

SUMMARY AND CONCLUSIONS

The present study uniquely identifies the shapes of Raman tensors for many localized vibrations of DNA. For example,

TABLE 8   Helix Raman tensors proposed for DNA duplexes

A DNA band (cm⁻¹)	$r_{1'}$ $(=r_{2'})$	B DNA band (cm⁻¹)	$r_{1'}$ $(= r_{2'})$
1667	−2.1	1669	−1.8
1577	−2.4	1578	−1.7
1339	−2.6	1339	−2.2
1257	−2.4	1257	−1.7

vibrational modes of the purines at 1339 and 1578 cm⁻¹ and of the pyrimidines at 1257 cm⁻¹ are characterized by highly anisotropic Raman tensors. In each case, one of the principal components of the Raman tensor is opposite in sign to the other two. On the other hand, for the purine 1487 cm⁻¹ mode, the tensor though anisotropic contains three principal components with the same algebraic sign. The tensors corresponding to the ring breathing vibrations of the base residues are intermediate in isotropic character, and the three principal tensor components exhibit the same sign. For the diagnostic PO_2^- symmetrical stretching vibration of the DNA backbone (1090–1100 cm⁻¹), the Raman tensor is intrinsically isotropic (Guan et al., 1993), and this trend is confirmed for both A and B DNA fibers. However, in crystalline Z DNA (Benevides et al., 1993) the tensor shape is subtly altered. The newly assigned furanose ring mode of the deoxyribose residue near 897 cm⁻¹ exhibits a Raman tensor that is characteristically isotropic.

How the Raman tensors may be deformed by intramolecular or intermolecular forces that vary with the local environment of DNA is an interesting problem. A survey of the present data suggests that stacking of the Watson-Crick base pairs tends to increase the anisotropy of Raman tensors associated with base residue vibrations. For example, Table 4 shows that the depolarization ratios of the bands at 1340 cm⁻¹ (G, A) and 1254 cm⁻¹ (C and T) are both appreciably higher in solutions of B DNA than in solutions of the nucleotide monomers (see Table 4). Higher depolarization ratios are also observed for base vibrations of double-stranded RNA in solution, (G.J. Thomas and J.M. Benevides, unpublished results). The only apparent exceptions to this trend have been noted for Z DNA (Benevides et al., 1993).

A major distinction between polarized Raman spectra of A and B DNA fibers is the larger magnitude of I_{bb}/I_{cc}, i.e., the greater experimental anisotropy, generally observed for bands due to base residue vibrations in the A conformer. Assuming that the base pairs of B DNA are more nearly perpendicular to the helix axis than are those of A DNA, it might be anticipated that larger intensity quotients would be observed in the B conformer. Since this is not the case, other factors must be considered. One important consideration is the higher crystallinity and greater degree of unidirectional orientation achievable for fibers of the A form than for fibers of the B form. This is consistent with fiber x-ray diffraction patterns reported for sodium salts of A and B DNA (Langridge et al., 1960; Fuller et al., 1965). The present results are also consistent with the local Raman tensors measured for the oriented single crystal of a Z DNA oligonucleotide, d(CGCGCG) (Benevides et al., 1993). For this crystal, a number of vibrations of G and C residues exhibit I_{bb}/I_{cc}

values that are even greater than those of corresponding base vibrations in the A DNA fiber examined here. Accordingly, each Raman tensor derived from the present fiber data should be considered as an effective tensor that incorporates the possible modulating effect of some orientational disorder.

Intrinsic structural heterogeneity in B DNA may also contribute to the lower anisotropies observed here for the B form fiber. Oligonucleotide crystal structures (reviewed by Kennard and Hunter, 1989) show that in B DNA the local geometry can vary substantially from one base pair to another and may be significantly dependent upon local sequence. Therefore, although the average plane of a base pair in B DNA is close to normal to the helix axis, each base pair is expected to exhibit greater deviations from parallel stacking (tilt, roll, and slide), as well as a greater deviation from coplanarity of paired bases (propeller twist and buckle), than is the case in either A or Z DNA. Thus, the local geometry in B DNA may play an important role in reducing the effective Raman anisotropies of in-plane base vibrations. Future studies will focus on determination of the Raman tensors of B DNA by measurement of polarized Raman spectra of oriented single crystals of B form oligonucleotides.

In summary, we propose classification of the local Raman tensors of fibers of A and B forms of DNA into the following specific categories:

1. Those that exhibit similarly high anisotropies in both A and B conformers. These are potential indicators of an oriented right-handed double helix in biological assemblies, but do not discriminate duplexes of the A and B genera from one another. Examples with assignments are the Raman bands at 1257 (C and T), 1339 (G and A), and 1578 cm⁻¹ (A and G).
2. Those that exhibit similarly low anisotropies in both A and B conformers. These are potentially valuable as internal intensity standards, particularly for polarized Raman spectroscopy of DNA and its complexes. Examples are the Raman bands at 900 (deoxyribose), 1093 (phosphates of B DNA), and 1101 cm⁻¹ (phosphates of A DNA).
3. Those that exhibit markedly different anisotropies in A and B conformers. These bands contain Raman tensors which can be exploited not only to identify right-handed double helical DNA, but also to distinguish the A and B conformations of DNA from one another. Potential candidates are the Raman bands at 666/682 (G), 731/729 (A), 753/750 (T), 784/784 (C), 807/836 (phosphodiester), 1419/1420 (deoxyribose), 1486/1487 (G and A) and 1667/1669 cm⁻¹ (T and G).

Confirmation and extension of the present conclusions through tensor determinations on oriented A and B DNA oligonucleotide single crystals is currently in progress.

nucleic acids. II. *Ab initio* calculation of the molecular force field and normal modes of dimethyl phosphate, *J. Am. Chem. Soc.* (submitted 1994).

REFERENCES

Arnott, S., and D. W. L. Hukins. 1972. Optimized parameters for *A* DNA and *B* DNA. *Biochem. Biophys. Res. Commun.* 47:1504–1510.

Aubrey, K. L., S. R. Casjens, and G. J. Thomas, Jr. 1992. Secondary structure and interactions of the packaged dsDNA genome of bacteriophage P22 investigated by Raman difference spectroscopy. *Biochemistry* 31: 11835–11842.

Barnes, A. J., M. A. Stuckey, and L. LeGall. 1984. Nucleic acid bases studied by matrix isolation vibrational spectroscopy: uracil and deuterated uracils. *Spectrochim. Acta* 40A:419–431.

Benevides, J. M., M. Tsuboi, A. H.-J. Wang, and G. J. Thomas, Jr. 1993. Local Raman tensors of double-helical DNA in the crystal: a basis for determining DNA residue orientations. *J. Am. Chem. Soc.* 115:5351–5359.

Brandes, R., A. Rupprecht, and D. R. Kearns. 1989. Interaction of water with oriented DNA in the A- and B-form conformations. *Biophys. J.* 56:683–691.

Brown, E. B., and W. L. Peticolas. 1975. Conformational geometry and vibrational frequencies of nucleic acid chains. *Biopolymers.* 14:1259–1271.

Delabar, J. M., and M. Majoube. 1978. Infrared and Raman spectroscopic study of 15N and D-substituted guanines. *Spectrochim. Acta.* 34A:129–140.

Erfurth, S. C., E. J. Kiser, and W. J. Peticolas. 1972. Determination of the backbone structure of nucleic acids and nucleic acid oligomers by laser Raman scattering. *Proc. Natl. Acad. Sci. USA.* 69:938–941.

Fuller, W., M. H. F. Wilkins, H. R. Wilson, and L. D. Hamilton. 1965. The molecular configuration of deoxyribonucleic acid. IV. X-ray diffraction study of the *A* form. *J. Mol. Biol.* 12:60–76.

Guan, Y., C. J. Wurrey, and G. J. Thomas, Jr. 1994. Vibrational analysis of nucleic acids. I. The phosphodiester group in dimethyl phosphate model compounds: $(CH_3O)_2PO_2^-$, $(CD_3O)_2PO_2^-$ and $(^{13}CH_3O)_2PO_2^-$. *Biophys. J.* 66:225–235.

Hartman, K. A., R. C. Lord, and G. J. Thomas, Jr. 1973. Structural studies of nucleic acids and polynucleotides by infrared and Raman spectroscopy. *In* Physico-Chemical Properties of Nucleic Acids, Vol. 2. J. Duchesne, editor. Academic Press, New York. 1–89.

Higgs, P. W. 1953. The vibration spectra of helical molecules. Infrared and Raman selection rules, intensities and approximate frequencies. *Proc. R. Soc. London.* A220:472–485.

Hirakawa, A. Y., H. Okada, S. Sasagawa, and M. Tsuboi. 1985. Infrared and Raman spectra of adenine and its ^{15}N and ^{13}C substitution products. *Spectrochim. Acta.* 41A:209–216.

Katahira, M., Y. Nishimura, M. Tsuboi, T. Sato, Y. Mitsui, and Y. Iitaka. 1986. Local and overall conformations of DNA double helices with the A·T base pairs. *Biochim. Biophys. Acta.* 867:256–267.

Kennard, O., and W. N. Hunter. 1989. Oligonucleotide structure: a decade of results from single crystal X-ray diffraction studies. *Q. Rev. Biophys.* 22:327–379.

Langridge, R., D. A. Marvin, W. E. Seeds, H. R. Wilson, C. R. Hooper, M. H. F. Wilkins, and L. D. Hamilton. 1960. The molecular configuration of deoxyribonucleic acid. II. Molecular models and their Fourier transforms. *J. Mol. Biol.* 2:38–64.

Li, T., D. H. Bamford, J. K. H. Bamford, and G. J. Thomas, Jr. 1993. Structural studies of the enveloped dsRNA bacteriophage φ6 of Pseudomonas syringae by Raman spectroscopy. I. The virion and its membrane envelope. *J. Mol. Biol.* 230:461–472.

Li, T., J. E. Johnson, and G. J. Thomas, Jr. 1993. Raman dynamic probe of hydrogen exchange in bean pod mottle virus: base-specific retardation of exchange in packaged ssRNA. *Biophys. J.* 65:1963–1972.

Li, Y., G. J. Thomas, Jr., M. Fuller, and J. King, 1981. Investigations of bacteriophage P22 by laser Raman spectroscopy. *Prog. Clin. Biol. Res.* 64:271–283.

Lord, R. C., and G. J. Thomas, Jr. 1967. Raman spectral studies of nucleic acids and related molecules. I. Ribonucleic acid derivatives. *Spectrochim. Acta.* 23A:2551–2591.

Nishimura, Y., K. Morikawa, and M. Tsuboi. 1974. Spectral difference of the A and B forms of deoxyribonucleic acid. *Bull. Chem. Soc. Jpn.* 47:1043–1044.

Nishimura, Y., M. Tsuboi, T. Sato, and K. Aoki, 1986. Conformation-sensitive Raman lines of mononucleotides and their use in a structure analysis of polynucleotides: guanine and cytosine nucleotides. *J. Mol. Struct.* 146:123–153.

Pilet, J., and J. Brahms. 1972. Dependence of *B–A* conformational change in DNA on base composition. *Nature New Biol.* 236:99–100.

Prescott, B., W. Steinmetz, and G. J. Thomas, Jr. 1984. Characterization of DNA secondary structure by Raman spectroscopy. *Biopolymers.* 23:235–256.

Puppels, G. J., C. Otto, J. Greve, M. Robert-Nicoud, D. J. Arndt-Jovin, and T. M. Jovin. 1994. Raman microspectroscopic study of low-pH-induced changes in DNA structure of polytene chromosomes. *Biochemistry.* 33: 3386–3395.

Shimanouchi, T., M. Tsuboi, and Y. Kyogoku. 1964. Infrared spectra of nucleic acids and related compounds. *Adv. Chem. Phys.* 7:435–498.

Small, E. W., and W. L. Peticolas. 1971. Conformational dependence of the Raman scattering intensities from polynucleotides. *Biopolymers.* 10: 69–88.

Stangret, J., and R. Savoie. 1992. Vibrational spectroscopic study of the interaction of metal ions with diethyl phosphate, a model for biological systems. *Can. J. Chem.* 70:2875–2883.

Susi, H., J. S. Ard, and J. M. Purcell. 1973. Vibrational spectra of nucleic acid constituents. II. Planar vibrations of cytosine. *Spectrochim. Acta.* 29A:725–733.

Sutherland, G. B. B. M., and M. Tsuboi. 1957. The infra-red spectrum and molecular configuration of sodium deoxyribonucleate. *Proc. Roy. Soc.* A239:446–463.

Szczesniak, M., M. J. Nowak, H. Rostkowska, K. Szczepaniak, W. B. Person, and D. Shugar. 1983. Matrix isolation studies of nucleic acid constituents. 1. Infrared spectra of uracil monomers. *J. Am. Chem. Soc.* 105:5969–5976.

Thomas, G. J. Jr. 1970. Raman spectral studies of nucleic acids. III. Laser-excited spectra of ribosomal RNA. *Biochim. Biophys. Acta.* 213:417–423.

Thomas, G. J. Jr. and D. A. Agard. 1984. Quantitative analysis of nucleic acids, proteins and viruses by Raman band deconvolution. *Biophys. J.* 46:763–768.

Thomas, G. J. Jr., J. M. Benevides, and B. Prescott. 1986. DNA and RNA structures in crystals, fibers and solutions by Raman spectroscopy with applications to nucleoproteins. *In* Biomolecular Stereodynamics, Vol. 4. R. H. Sarma, and M. H. Sarma, editors. Adenine Press, Guilderland, NY. 227–254.

Thomas, G. J. Jr., and J. M. Benevides. 1985. An A-helix structure for poly(dA-dT)·poly(dA-dT). *Biopolymers.* 24:1101–1105.

Thomas, G. J. Jr., and M. Tsuboi. 1993. Raman spectroscopy of nucleic acids and their complexes. *Adv. Biophys. Chem.* 3:1–70.

Thomas, G. J. Jr., and A. H.-J. Wang. 1988. Laser Raman spectroscopy of nucleic acids. *Nucleic Acids Mol. Biol.* 2:1–30.

Toyama, A., Y. Takino, H. Takeuchi, and I. Harada. 1993. Ultraviolet resonance Raman spectra of ribosyl C(1')-deuterated purine nucleosides: evidence of vibrational coupling between purine and ribose rings. *J. Am. Chem. Soc.* 115:11092–11098.

Tsuboi, M. 1957. Vibrational spectra of phosphite and hypophosphite anions, and the characteristic frequencies of PO_3^{2-} and PO_2^- groups. *J. Am. Chem. Soc.* 79:1351–1354.

Tsuboi, M., T. Ikeda, and T. Ueda. 1991. Raman microscopy of a small uniaxial crystal: tetragonal aspartame. *J. Raman Spectrosc.* 22:619–626.

Tsuboi, M., Y. Nishimura, A. Y. Hirakawa, and W. L. Peticolas. 1987. Resonance Raman spectroscopy and normal modes of the nucleic acid bases. *In* Biological Applications of Raman Spectroscopy: Resonance Raman Spectra of Polyenes and Aromatics, Vol. 2. T. G. Spiro, editor. Wiley-Interscience, New York. 109–179.

Tsuboi, M., S. Takahashi, and I. Harada. 1973. Infrared and Raman spectra of nucleic acids: vibrations in the base residues. *In* Physico-Chemical Properties of Nucleic Acids, Vol. 1. J. Duchesne, editor. Academic Press, New York, 92–143.

Tsuboi, M., T. Ueda, K. Ushizawa, Y. Sasatake, A. Ono, M. Kainosho, and Y. Ishido. 1994. Assignments of the deoxyribose vibrations: isotopic thymidine. *Bull. Chem. Soc. Jpn.* 67:1483–1484.

Ueda, T., K. Ushizawa, and M. Tsuboi. 1993. Depolarization of Raman scattering from some nucleotides of RNA and DNA. *Biopolymers.* 33:1791–1802.

Ueda, T., K. Ushizawa, and M. Tsuboi. 1994. Local Raman tensors in adenosine triphosphoric acid. *Spectrochim. Acta.* 50A:1661–1674.